Journal of Physics: Conference Series **234** (2010) 012015 doi:10.1088/1742-6596/234/1/012015

Pulsed laser deposition of niobium thin films for in-situ device fabrication and their superconducting properties

V Grosse[1], C Pansow[1], A Steppke[1,2], F Schmidl[1], A Undisz[3], M Rettenmayr[3], A Grib[1,4] and P Seidel[1]

[1] Institut für Festkörperphysik, Friedrich-Schiller-Universität Jena, Helmholtzweg 5, 07743 Jena, Germany
[2] MPI für chemische Physik fester Stoffe, Nöthnitzer Straße 40, 01187 Dresden, Germany
[3] Institut für Materialwissenschaft und Werkstoffkunde, Friedrich-Schiller-Universität Jena, Löbdergraben 32, 07743 Jena, Germany
[4] Physics Department, V. N. Karazin Kharkiv National University, 61077 Kharkiv, Ukraine

E-mail: veit.grosse@uni-jena.de

Abstract. Here, we studied the crystallographic and superconducting properties of niobium thin films grown by pulsed laser deposition. Depending on laser fluence our samples showed a critical temperature of up to 8.4 K and critical current densities of $3.0 \cdot 10^6$ A/cm^2 at 4.2 K. X-ray diffraction measurements and TEM images suggest a granular structure with a preferred orientation of the (110) lattice plane parallel to the substrate surface. The superconducting properties of our films are significantly influenced by this granularity and the oxygen content in the film. We discuss the temperature dependence of the critical current density in the framework of an crossover from Ginzburg-Landau to Ambegaokar-Baratoff type behaviour. According to this the current transport is mainly dominated by Josephson-tunnelling in a granular network.

Keywords: Niobium, Pulsed Laser Deposition, granular superconductor, Josephson effect

1. Introduction

High quality superconducting Niobium (Nb) thin films with critical temperatures of $\gtrsim 9.2$ K are commonly grown by electron beam evaporation or sputtering under ultra high vacuum (UHV) conditions. They are typically applied to fabricate RF cavities and Josephson junctions in superconducting electronics [1–4]. In recent years new concepts of designing Josephson junctions lead to a growing number of applications of Nb films in hybrid systems. Exemplarily we would like to refer to the combination with carbon nanotubes (CNTs) as weak link [5] or with high-T_C superconductors such as $YBa_2Cu_3O_{7-x}$ for Josephson junctions showing a non-zero phase difference in the ground state (e.g. π-junctions) [6–10]. In the same way Nb can also be used as a typical s-wave superconductor to test for the wave function symmetry of new superconducting materials [11]. Typically, each particular layer of these systems is grown utilising different appropriate deposition techniques requiring *ex-situ* processing or complex deposition chamber concepts. In the former case special measures have to be taken to ensure clean interfaces.

Against this background utilising pulsed laser deposition (PLD) to grow Nb thin films may provide a variety of advantages to fabricate hybrid systems. There are almost no limitations concerning the choice of the material to deposit. In particular PLD proved very successful in growing complex materials such as high-T_C superconductors [12]. It therefore offers the flexibility

to fabricate high quality multi-layer systems without the need to break the vacuum cycle. Furthermore, it is expected that higher ionisation states and energies of the evaporated particles could beneficially influence the electronic mean free path and thus improve film quality [13]. However, the pulsed laser deposition of metals (especially those with high melting temperatures) is challenging because of low optical absorption depths and high thermal diffusion lengths. For these materials extremely high ionisation and particle energies are expected, accompanied by low growth rates, a high deposition threshold and the tendency to produce high droplet densities [14].

Haindl *et al.* [15–17] demonstrated the applicability of PLD grown Nb films in epitaxial multilayer systems. In contrast to this we will focus on the discussion of the structural and superconducting properties of non-epitaxial Nb films. We restricted ourselves to the deposition at room temperature to limit damaging of preliminarily grown layers at elevated substrate temperatures.

2. Sample Preparation and Morphology

Our Nb films were grown on thermally oxidised Si (001) substrates. This substrate material is of particular interest in connection with the growth and wiring of CNTs. It is known that Si surfaces inhibit, whereas SiO_2 surfaces advance CNT growth [18, 19]. For subsequent electrical characterisation we applied a photolithographic lift-off mask to pattern micro-bridges featuring widths in the range of 2 to 20 μm and a length of 1 mm. This structure allows temperature dependent measurements of current-voltage characteristics and the dc-resistance in a standard four-probe method.

For deposition the vacuum chamber was evacuated to a residual pressure of less than $2.0 \cdot 10^{-5}$ Pa. We used a KrF excimer laser with a wave length of 248 nm and a pulse duration of 25 ns at a repetition rate of 10 Hz. The laser pulse was focused onto a Nb target (99.99% purity) to a spot size of approximately $1.5 \times 3\,\mathrm{mm}^2$. Contaminations of the target surface were removed by ablating target material for at least 15 min before deposition. The distance between target and substrate was 3 cm. To ensure an uniform target erosion and to reduce the droplet density the laser spot was swept across the target. By additionally polishing the target surface we were able to reduce the droplet density to $10^6\,\mathrm{cm}^{-2}$.

Figure 1 shows the dependence of the growth rate on laser fluence. From this we can estimate an ablation threshold of $(5.7 \pm 0.5)\,\mathrm{Jcm}^{-2}$. This value is almost identical to the vapour production threshold found by Rodrigues *et al.* [20] using a hydrogen bromide in discharge copper laser to ablate Nb. Best results with respect to the superconducting properties we realised at fluences of at least $7.5\,\mathrm{Jcm}^{-2}$ and the corresponding growth rate of (40 ± 5) nm/min. We address this fact to a reduced oxygen incorporation from the residual gas in the vacuum chamber at high growth rates. It should be noted that in our set-up we were not able to achieve laser fluences of more than $8.9\,\mathrm{Jcm}^{-2}$.

X-ray diffraction measurements shown in figure 2 suggest a granular morphology with a preferred orientation of the (110) lattice plane parallel to the substrate surface. From the profile width of the Nb (110) reflection we calculated an average grain size of (10 ± 1) nm using the Scherrer formula [21]. The position of this reflection is slightly shifted to lower Bragg-angles than expected for bulk Nb. This increase in the lattice plane spacing might be originated by either stress between individual grains or by the formation of metallic or insulating Nb oxides. A similar behaviour has been observed for sputter deposited Nb films [22]. Especially, the solid solution of oxygen in Nb and the formation of tetragonal NbO_6 ($a = 3.389$ Å and $c = 3.276$ Å) is known to produce the observed lattice expansion [23].

Transmission electron microscopy (TEM) images mainly support this interpretation of the X-ray data, see figure 3. They confirm that our films consist of crystalline grains having a size of a few nanometers with no indication for amorphous regions. Typical lattice spacings extracted from

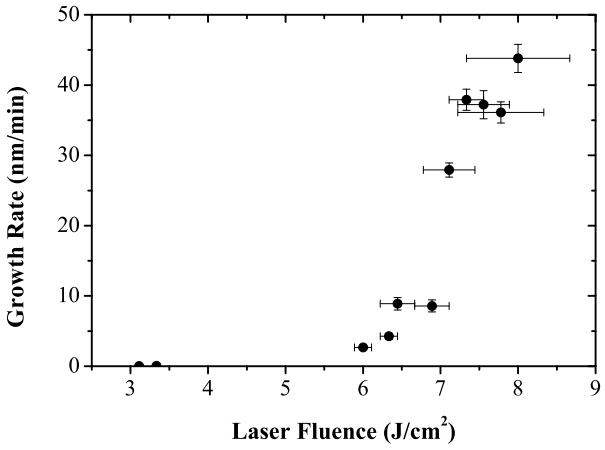

Figure 1. Growth rate versus laser fluence. During deposition the laser fluence reduces due to a growing Nb film on the debris protection used to cover the quartz window. The error bars indicate the difference between the laser fluence before and after deposition.

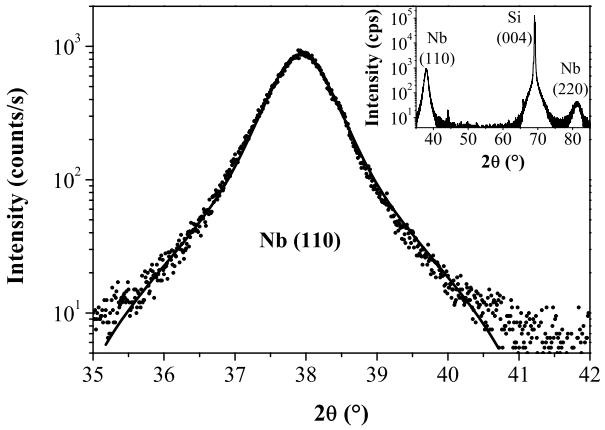

Figure 2. X-ray diffraction pattern for a 650 nm thick Nb film deposited at a laser fluence of $8.2\,\mathrm{Jcm^{-2}}$. Broad Nb (110) and Nb (220) reflections with a full width at half maximum of 0.9° indicate a granular structure. Using the Scherrer formula we calculated an average grain size of (10 ± 1) nm.

these images lie in the range between 2.38 and 2.41 Å which correspond to the ⟨110⟩-direction of NbO_6. Another prominent lattice spacing of (4.18 ± 0.04) Å, that can be found in the upper left region of figure 3b, can be associated to the ⟨100⟩-direction of NbO [24]. However, we cannot draw conclusions about the initial composition of the film after deposition since our samples were exposed to air after preparation for TEM measurements. Thus, an additional oxygen uptake is likely which explains that no pure Nb could be identified from these images.

3. Superconducting Properties

To characterise our samples we concentrated on the analysis of the critical temperature T_C and critical current density j_C. We measured the temperature dependence of the resistance at a bias current of $10\,\mu$A. We defined T_C to be the midpoint and the transition width to be the difference

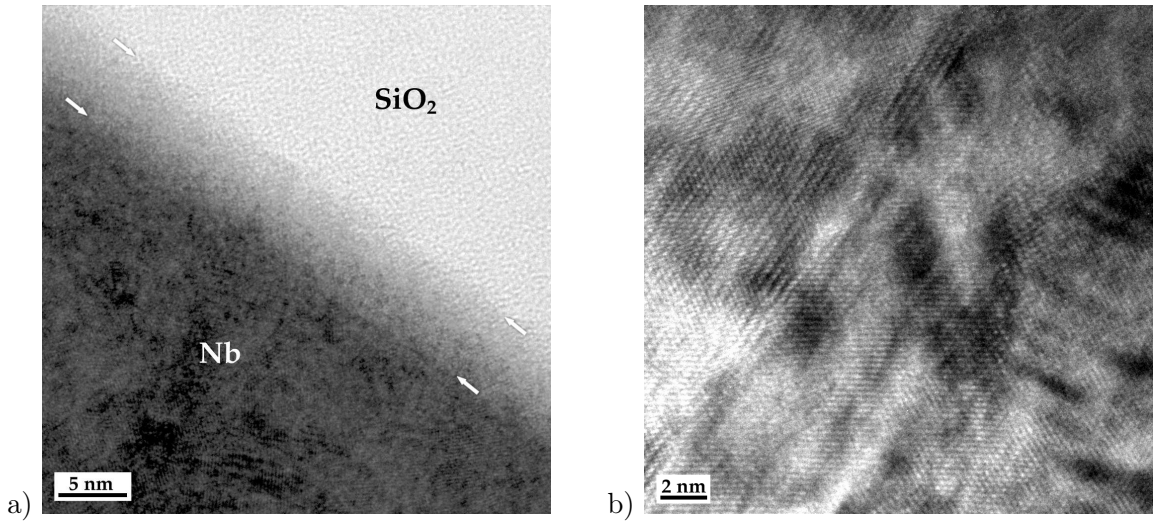

Figure 3. Bright field TEM images of a typical Nb film grown by PLD: a) Interface between the amorphous SiO_2 substrate and the granular Nb film. There is a noticeable transition region of a few nm thickness potentially caused by the impact of high energetic Nb particles from the laser plasma (marked with arrows). b) Higher resolution image of the Nb film showing crystallites with different orientations. Dark and bright regions are an indication for internal strain.

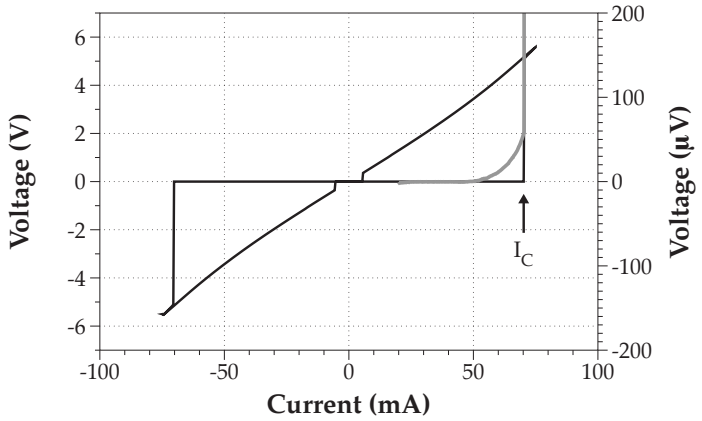

Figure 4. I-V characteristic of a 650 nm thick sample at 4.7 K ($T_C = 8.4$ K). Black line (right voltage scale): Full hysteretic characteristic caused by self heating in the resistive state. Gray line (right voltage scale): Measurement with higher accuracy showing the typical behaviour close I_C caused by flux creep or thermally activated phase slippage.

between the corresponding temperatures of 10% and 90% of the normal state resistance at 10 K. From current-voltage characteristics we determined the critical current I_C to be the current value for which the film switches to the resistive state, i.e., voltages generated by flux creep or thermal effects are exceeded (see figure 4). From this we calculated $j_C = I_C/wd$, where w and d are the width and the thickness of the micro-bridge, respectively.

Critical temperatures of our samples show a distinct dependence on film thickness, see figure 5. A minimum thickness of about 100 nm is necessary to obtain superconducting Nb films. In the current setup these findings have to be addressed mainly to oxidation from residual gas

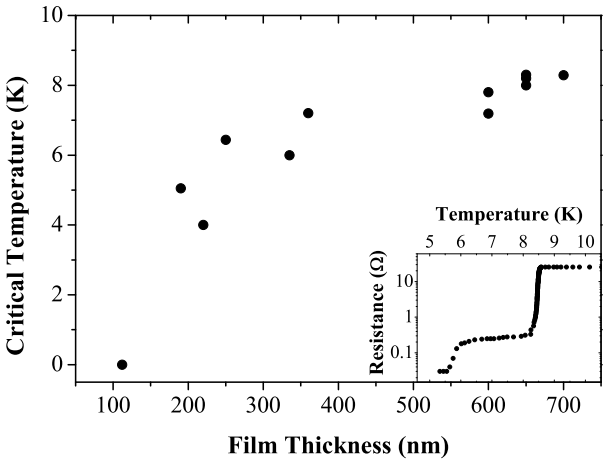

Figure 5. Dependence of the critical temperature on film thickness. The inset shows the $R(T)$ characteristic of a sample with $T_C = 8.4\,K$ and a film thickness of 650 nm close to the superconducting phase transition.

during film deposition. The minimum background pressure of 10^{-5} Pa we obtained in the our deposition chamber is to high to grow high quality Nb films. Thus, incorporation of residual gases can only be limited by increasing deposition rates. Additionally, high particle energies within the laser generated plasma may advance surface damaging and reduction of the substrate material favouring formation Nb oxides. This effect becomes less significant the more material is deposited, but can result in a non-superconducting layer at the interface between Nb film and substrate (figure 3a). Oxygen transport along defects such as grain boundaries after deposition can in principle not be excluded. However, we did not observe a significant deterioration of the superconducting properties of samples stored for two weeks in air compared those measured directly after deposition. There are other influences which should be considered for reducing the critical temperature of our films, e.g., proximity [25] or grain size effects [26]. Based on these considerations significant improvements in film quality can be obtained by growing the film under UHV condition. Furthermore, introducing a reducing gas (e.g. H_2) during deposition could minimise particle energy and prevent oxidation of the growing film.

The inset of figure 5 shows the temperature dependence of the resistance near the phase transition. It clearly exhibits a food structure which can be produced by thermally activated phase slippage in superconducting tunnelling structures [27, 28]. To reproduce the $R(T)$-characteristic one has to assume varying critical temperatures over the whole system of grains. For our films this implies that tunnelling between superconducting Nb grains has to be considered to describe current transport through the film. This can, in particular, be demonstrated by analysing the temperature dependence of the critical current density.

The following results in this section were taken from the sample showing the highest critical temperature of $T_C = 8.4\,K$ and a transition width $\Delta T_C \approx 0.1\,K$. The $j_C(T)$-characteristics differ significantly from observations made by other groups which report a Ginzburg-Landau type dependence [29, 30] given by [31]:

$$j_C(T) = j_C^0(1-t^2)^{3/2}(1+t^2)^{1/2}\ , \tag{1}$$

where $t = T/T_C$. To explain this deviation we applied a model developed by Clem *et al.* [32] considering Josephson-coupling between grains. For our films we propose a lattice (or network) consisting of superconducting Nb grains separated by Nb oxide barriers. For such a model system

the critical current density can be expressed in the form [32]:

$$j_{\mathrm{C}}(T) = \frac{I_0(T)}{A} g(\epsilon) \ , \tag{2}$$

where A is the cross section of the micro-bridge and $g(\epsilon) = f_{\mathrm{m}}^2 \sin\phi_{\mathrm{m}}$ is a factor reducing the critical current below the Ambegaokar-Baratoff maximum Josephson current $I_0(T)$ caused by the gap suppression in the presence of a supercurrent. The factor f_{m}^2 is given by [32]:

$$f_{\mathrm{m}}^2 = 1 - \epsilon(1 - \cos\phi_{\mathrm{m}}) \ , \tag{3}$$

with

$$\cos\phi_{\mathrm{m}} = \frac{(1 - 2\epsilon + 9\epsilon^2)^{1/2} - 1 + \epsilon}{4\epsilon} \tag{4}$$

and $\epsilon = E_{\mathrm{J}}/2E_{\mathrm{S}}$ is half the ratio between the Josephson-coupling energy $E_{\mathrm{J}} = (\hbar/2e)I_0$ and the superconducting condensation energy $E_{\mathrm{S}} = H_{\mathrm{C}}^2 V/8\pi$ (H_{C} is the critical magnetic field and V is the grain volume).

Barriers between grains cannot be assumed to be ideal. In particular, metallic or even superconducting Nb oxides can form interlayers between the grain and the actual barrier. In this case it has been shown that proximity effects can influence the temperature dependence of the critical Josephson current significantly [33]. Proximity induced modifications of the electronic density of states near the Fermi energy $N(0)$ lead to a distribution of gap parameters determining the maximum Josephson current. To simplify this problem we used the Ambegaokar-Baratoff expression for tunnelling between two dissimilar superconductors [34, 35]:

$$I_0(T) = \frac{\pi\Delta_1(T)\Delta_2(T)}{eR_{\mathrm{N}}\beta} \sum_{j=0,\pm1,\pm2,\ldots} \left\{ \left[\omega_j^2 + \Delta_1^2(T)\right] \left[\omega_j^2 + \Delta_2^2(T)\right] \right\}^{-1/2} \ . \tag{5}$$

Here $\omega_j = (\pi/\beta)(2j+1)$ is the imaginary part of the poles of the complex Fermi function and $\beta = 1/k_{\mathrm{B}}T$. Using the BCS relations [36] and performing the rearrangements as described in [32] we now find for the normalised Josephson-coupling energy:

$$\begin{aligned} \epsilon(T) = \epsilon_0 \frac{T/T_{\mathrm{C}}}{\left[H_{\mathrm{C}}(T)/H_{\mathrm{C}}(0)\right]^2} \Delta_1(T)\Delta_2(T) \\ \cdot \sum_j \left\{ \left[\omega_j^2 + \Delta_1^2(T)\right] \left[\omega_j^2 + \Delta_2^2(T)\right] \right\}^{-1/2} \ , \end{aligned} \tag{6}$$

where

$$\epsilon_0 = 3.32 \frac{\hbar k_{\mathrm{B}}}{e^2 R_{\mathrm{N}} \gamma T_{\mathrm{C}} V} \ . \tag{7}$$

Here R_{N} is the normal state resistance and $\gamma = \frac{2}{3}\pi N(0) k_{\mathrm{B}}^2$.

The results of the analysis according to (2)–(6) for two micro-bridges are shown in figure 6. Except for temperatures close to T_{C} our experimental data follows the Ambegaokar-Baratoff critical current dependence for tunnelling between two superconductors. From the temperature dependence of the normalised Josephson-coupling energy we can determine a crossover temperature $T_{\mathrm{X}}/T_{\mathrm{C}} = 0.97 \pm 0.01$ ($\epsilon(T_{\mathrm{X}}) = 1$) above which gap suppression is dominant [32]. The critical current then approaches a Ginzburg-Landau type behaviour. We obtain best fits to our data using the model parameters $\Delta_1(0) = 1.2\,\mathrm{meV}$, $T_{\mathrm{C},1} = 9.2\,\mathrm{K}$ and $\Delta_2(0) = 0.7\,\mathrm{meV}$, $T_{\mathrm{C},2} = 8.4\,\mathrm{K}$.

For bulk Nb, tunnelling measurements give a relation between the energy gap at zero temperature and the critical temperature of $2\Delta(0)/k_{\mathrm{B}}T_{\mathrm{C}} = 3.60 \ldots 3.96$ [37]. Compared to

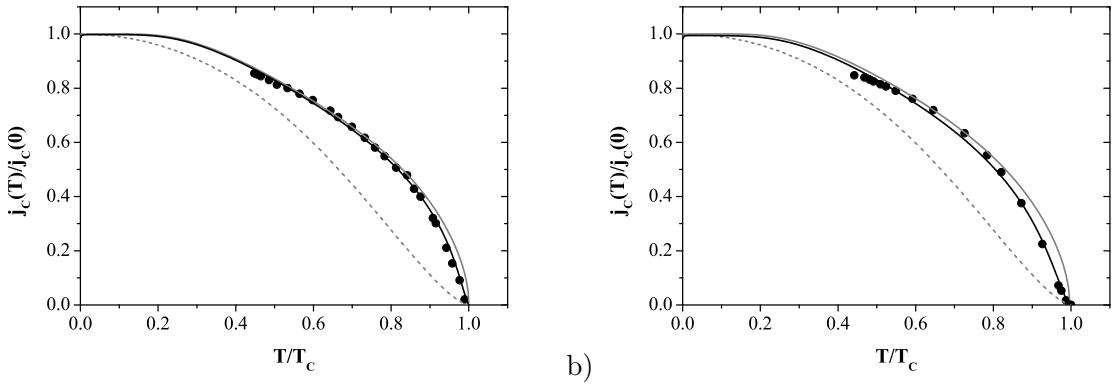

Figure 6. Reduced critical current density versus reduced temperature. Experimental data of two different micro-bridges with a width of a) 3 μm and b) 4 μm of the same sample are plotted with black dots. The grey lines represent the Ambegaokar-Baratoff maximum Josephson current (solid) and the Ginzburg-Landau critical current density (dashed). The black lines are fits to the experimental data according to (2)–(6).

this relation the values we determined from our measurements using the introduced model are too small. But as we pointed out before, tunnelling in our granular Nb films is influenced by proximity effects. Such systems have been discussed in detail and are known to show a reduced effective energy gap which is comparable to the gaps we observed [33, 38]. In this case the bulk relation for $\Delta(0)$ does not hold .

4. Summary

In this paper we demonstrated the potential of growing superconducting Nb thin films by PLD. The films showed a nano-crystalline granular structure which has a significant influence on the dependence of the critical current on temperature. We successfully applied a model describing our films as network of Josephson-coupled grains. Thereby, proximity effects between Nb and its oxides have to be considered leading to a distribution of the gap parameter and the critical temperature over the whole of grains. Based on these results the application of PLD grown Nb films in hybrid systems appears promising. However, oxidation has to be limited by growing the films under UHV conditions and subsequently applying a passivation layer. This will be part of further investigations on the properties of PLD grown Nb films.

References

[1] Benvenuti C, Circelli N and Hauer M 1984 *Applied Physics Letters* **45** 583–584

[2] Bemporad E, Carassiti F, Sebastiani M, Lanza G, Palmieri V and Padamsee H 2008 *Superconductor Science & Technology* **21** 125026

[3] Gubin A I, Il'in K S, Vitusevich S A, Siegel M and Klein N 2005 *Physical Review B* **72** 064503

[4] Kohlstedt H, Gundlach K H and Schneider A 1991 *IEEE Transactions On Magnetics* **27** 3149–3152

[5] Pallecchi E, Gaass M, Ryndyk D A and Strunk C 2008 *Applied Physics Letters* **93** 072501

[6] Komissinskiy P, Ovsyannikov G A, Constantinian K Y, Kislinski Y V, Borisenko I V, Soloviev I I, Kornev V K, Goldobin E and Winkler D 2008 *Physical Review B* **78** 024501

[7] Smilde H J H, Ariando, Blank D H A, Hilgenkamp H and Rogalla H 2004 *Physical Review B* **70** 024519

[8] Smilde H J H, Ariando, Rogalla H and Hilgenkamp H 2004 *Applied Physics Letters* **85** 4091–4093

[9] Ortlepp T, Ariando, Mielke O, Verwijs C J M, Foo K F K, Andreski A, Rogalla H, Uhlmann F H and Hilgenkamp H 2007 *IEEE Transactions On Applied Superconductivity* **17** 659–663

[10] Kawabata S, Golubov A A, Ariando, Verwijs C J M, Hilgenkamp H and Kirtley J R 2007 *Physical Review B* **76** 064505

[11] Parker D and Mazin I I 2009 *Physical Review Letters* **102** 227007

[12] Fogarassy E and Lazare S (eds) 1992 *Laser Ablation of Electronic Materials* (North-Holland)

[13] Catani L, Cianchi A, Lorkiewicz J, Tazzari S, Langner J, Strzyzewski P, Sadowski M, Andreone A, Cifariello G, Di Gennaro E, Lamura G and Russo R 2006 *Physica C-Superconductivity And Its Applications* **441** 130–133

[14] Willmott P R and Huber J R 2000 *Reviews Of Modern Physics* **72** 315–328

[15] Haindl S, Neu V, Schultz L and Holzapfel B 2007 *Physica C - Superconductivity and Its Applications* **460** 1390–1391

[16] Haindl S, Weisheit M, Neu V, Schultz L and Holzapfel B 2007 *Physica C - Superconductivity and Its Applications* **463** 1001–1004

[17] Haindl S, Weisheit M, Thersleff T, Schultz L and Holzapfel B 2008 *Superconductor Science & Technology* **21** 045017

[18] Wei B Q, Vajtai R, Jung Y, Ward J, Zhang R, Ramanath G and Ajayan P M 2002 *Nature* **416** 495–496

[19] Zhang Z J, Wei B Q, Ramanath G and Ajayan P M 2000 *Applied Physics Letters* **77** 3764–3766

[20] Rodrigues N A S, Giao M A P, Silveira C A B, Riva R and Schwab C 2002 *Applied Surface Science* **200** 68–75

[21] Warren B E 1969 *X-Ray Diffraction* (Dover Publications, New York)

[22] Saito Y and Anayama T 1975 *Journal of Low Temperature Physics* **21** 169–177

[23] Halbritter J 1987 *Applied Physics A-Materials Science & Processing* **43** 1–28

[24] Logacheva V A, Divakova N A, Tikhonova Y A, Dolgopolova E A and Khoviv A M 2007 *Inorganic Materials* **43** 1230–1234

[25] Prokhorov V G 1998 *Low Temperature Physics* **24** 410–413

[26] Bose S, Raychaudhuri P, Banerjee R, Vasa P and Ayyub P 2005 *Physical Review Letters* **95** 147003

[27] Ambegaokar V and Halperin B I 1969 *Physical Review Letters* **22** 1364–1366

[28] Gross R, Chaudhari P, Dimos D, Gupta A and Koren G 1990 *Physical Review Letters* **64** 228–231

[29] Il'in K, Siegel M, Semenov A, Engel A and Hubers H W 2005 *Physica Status Solidi C - Conferences and Critical Reviews* **2** 1680–1687

[30] Kuriki S and Gundlach K H 1979 *Journal Of Applied Physics* **50** 3514–3517

[31] Skocpol W J, Beasley M R and Tinkham M 1974 *Journal Of Applied Physics* **45** 4054–4066

[32] Clem J R, Bumble B, Raider S I, Gallagher W J and Shih Y C 1987 *Physical Review B* **35** 6637–6642

[33] Seidel P and Richter J 1980 *Physica Status Solidi B-Basic Research* **99** 607–613

[34] Ambegaokar V and Baratoff A 1963 *Physical Review Letters* **10** 486–489

[35] Ambegaokar V and Baratoff A 1963 *Physical Review Letters* **11** 104

[36] Bardeen J, Cooper L N and Schrieffer J R 1957 *Physical Review* **108** 1175–1204
[37] Carbotte J P 1990 *Reviews of Modern Physics* **62** 1027–1157
[38] Koehler H J and Seidel P 1980 *Physica Status Solidi B - Basic Research* **99** K51–K54